Natural Resources for Human Health
eISSN: 2583-1194

Original Research

Received 16 May 2026
Revised 18 June 2026
Accepted 30 June 2026

Natural Resources for Human Health 2026, Vol. 6 (4s): 466–474

KEYWORDS:
Indole Schiff base, multi-target inhibitors, breast cancer, hDHFR, carbonic anhydrase IX/XII

Novel Indole-PABA hybrids as dual hDHFR and CA IX/XII breast cancer inhibitors

Abbas H. Abdulsada[1], Monther F. Mahdi[2], Fouad A.A. Al-Saady[3]

[1]Department of Pharmaceutical Chemistry, College of Pharmacy, Mustansiriyah University, Baghdad, Iraq, E-mail: abbas_hamid@uomustansiriyah.edu.iq, ORCID: https://orcid.org/0000-0002-7621-0245
[2]Department of Pharmaceutical Chemistry, College of Pharmacy, Mustansiriyah University, Baghdad, Iraq, E-mail: dr.monther.f71@uomustansiriyah.edu.iq, ORCID: https://orcid.org/0000-0002-2069-4121
[3]Department of Pharmaceutical Chemistry, College of Pharmacy, Mustansiriyah University, Baghdad, Iraq, E-mail: dr.fouad.a@uomustansiriyah.edu.iq, ORCID: https://orcid.org/0000-0002-1176-4298
Corresponding author: Abbas H. Abdulsada, E-mail: abbas_hamid@uomustansiriyah.edu.iq

ABSTRACT:

Background: A library of 8 novel indole-PABA hybrids was designed/ synthesized as hDHFR/CA IX XII dual inhibitors for breast cancer therapy.

Aim: the aim of the study was to investigate the synthesized indole-PABA hybrids as potential hDHFR/CA IX XII dual inhibitors for breast cancer therapy.

Materials and Methods: Target compounds were synthesized by Schiff base method, amide coupling and alkaline hydrolysis methods and confirmed their structures by IR and NMR spectral analysis. Most compounds showed favorable drug-like properties, according to in silico ADMET predictions, and most compounds met Lipinski's Rule of Five, DFT calculations provided insights into electronic reactivity of the compounds depending upon substituents. This in vitro MTT activity against breast cancer cell lines (MDA-MB231 and MCF-7) indicated time-dependent antiproliferative activity.

Results: The most potent compound against MDA-MB-231 cells (IC_{50} = 19.93 μM at 72 h) was compound 3h (5-bromo-3-chloro derivative), which was more active than the reference compound acetazolamide (IC_{50} = 24.98 μM at 72 h), compound 3f (5-bromo-2-methyl derivative) being most active against MCF-7 cells (IC_{50} = 28.56 μM at 72 h). These were confirmed by percentages of cells which are being killed, with 3h and 3b showing the highest efficacy against MDA cells.

Conclusion: The results reveal that there are three compounds 3h, 3b, and 3f, which are potential lead candidates for further optimization and mechanistic studies as multi-target anticancer agents.

INTRODUCTION

Breast cancer is a daunting worldwide health challenge, which is among the most diagnosed type of malignancy and the most frequent cause of cancer-related deaths in women all over the globe [1-2]. The number of new cases and deaths due to female breast cancer was 2.3 million and 670,000 in the world in 2022, and the incidence rates are still increasing in half of the countries

studied [3]. It has a considerable biological heterogeneity, and molecular subtypes are determined by the presence of receptors to hormones (estrogen and progesterone) and human epidermal growth factor receptor 2 (HER2) that are essential in informing treatment choice [1, 4]. Its etiology involves a complex interaction between genetic factors, including BRCA mutations, hormonal factors, lifestyle choices and reproductive patterns, with emerging new data suggesting that estrogens and progestogens have a responsibility in the pathogenesis of this disease [5-6]. The treatment approaches have changed significantly, and localized treatment (surgery and radiotherapy) has become the foundation of early-stage disease, supplemented by systemic treatment (chemotherapy, endocrine therapy, targeted agents, and tumor biology-based immunotherapy) [7-8]. Interestingly, there has been recent advances in treating triple-negative breast cancer (TNBC), an offensive form of breast cancer lacking these receptors, with the introduction of immunotherapy and PARP inhibitors, but it remains a serious therapeutic challenge [9]. Although there have been improvements in early diagnosis and targeted therapies, disparities in incidence and mortality continue to exist all over the world, making it essential to further investigate new therapeutic targets and provide equal access to care [10]. Multi-target drugs have become an appealing approach in oncology, in response to the natural complexity and redundancy of signaling networks that give rise to tumor progression and drug resistance. In contrast to traditional single-target agents, the compounds seek to simultaneously target several disease-relevant pathways, which have possibilities of superior efficacy and diminished toxicity [10]. The rational design of such agents is being increasingly rationalized faster due to systems pharmacology and machine learning, and allows predicting polypharmacology and discovering new multi-target directed ligands [12-13]. An example of this is that in the past few years, multi-target LSD1 inhibitive are going through clinical trials, and steroidal aromatase inhibitors, which also inhibit the estrogen and androgen receptors in treating breast cancer are this year [14-15]. Moreover, the combination of drug repurposing and polypharmacology is a synergistic technology to identify efficient multi-target therapeutics using already existing compounds [16]. Taken together, these approaches promise a new era of anti-cancer agents able to address the complexity of malignancy. The human dihydrofolate reductase (hDHFR) is a candidate anticancer target since its inhibition interferes with the mechanism of DNA synthesis and tumor growth. Although methotrexate has been clinically successful, resistance and selectivity problems remain ongoing motivations to discover more hDHFR inhibitors [17-18]. Concurrently, the carbonic anhydrase (CA) IX and XII isoforms have proved to be promising antitumor target. CA IX is a hypoxic and poor prognosis tumor markers in breast cancer [19-20] and CA XII is also overexpressed in diverse tumors. Both CA IX and CA XII inhibition have the potential to disrupt the acidic microenvironment that favors the progression of cancer (20). In turn, a combination of co-targeting hDHFR with CA IX and CA XII is a promising multi-target mode of therapy. In this direction, we have created eight molecular hybrids of indole-PABA (para-aminobenzoic acid) which is a potential hDHFR, CA IX and CA XII inhibitor.

MATERIALS AND METHODS

Materials and apparatus

The melting points of the new compounds were determined on an electric melting point apparatus (Stuart) with an open-glass capillary tube (uncorrected) at the University of Babylon. Infrared (IR) spectra were measured on a Shimadzu FT-IR spectrometer with KBr disks. Nuclear magnetic resonance (NMR) spectra were recorded on a Bruker 400.13 MHz for ^{1}H and 100.62 MHz for ^{13}C NMR spectrometer at the University of Tehran. The chemicals 4-aminobenzoic acid, 4-amino-2-methylbenzoic acid, 4-amino-2-methoxybenzoic acid, 4-amino-3-chlorobenzoic acid, indole-3-carboxaldehyde and 5-bromoindole-3-carboxaldehyde were purchased from Baoji Guokang Bio-Technology Co., Ltd.

Synthesis methodology

General method for the synthesis of 4-(((1H-indol-3-yl)methylene) amino)benzoic acid derivatives (1a-1h)

A mixture of indole-3-carboxaldehyde or 5-bromoindole-3-carboxaldehyde 2 mmol and a few drops of glacial acetic acid in ethanol 20 mL was stirred at 70°C for 5 min. The primary amine (para-ABA, 2-methyl-, 2-methoxy-, or 3-chloro-para-ABA; 2 mmol) was added in small portions into the solution and the mixture was refluxed at 80°C (692 F) in EtOH (15 mL), which was the target solvent, and it was monitored by TLC. The Schiff base indole product was filtered, washed with cold ethanol (3x) and dried after cooling to 0 Degree Celsius. Purification by recrystallization of the crude product was done in hot methanol or ethanol, based on solubility. In short, the crude solid was dissolved in at least boiling solvent, allowed to cool to room temperature, and put into an ice bath (0-5°C) to crystallize. The crystals were purified, filtered, washed using cold solvent and dried, yielding products 1a-1h [21].

Natural Resources for Human Health
eISSN: 2583-1194

General method for the synthesis of diethyl (4-(((1H-indol-3-yl) methylene) amino) benzoyl) glutamate (2a-2h)

Indole–PABA Schiff base intermediates (1a–1h, 1 equiv, 2 mmol) were dissolved in DCM with a stir bar, with the addition of small amounts THF co-solvent if necessary. HOBt (1 equiv, 2 mmol), EDC (1 equiv, 2 mmol) and then glutamate diethyl ester (1 equiv, 2 mmol) and DIPEA (1.5-2 equiv, 3-4 mmol) were added and the reaction was cooled to 0°C and stirred for 15 min. The reaction was allowed to stir at rt for 20-24 h (as monitored by TLC). Solvents were removed, residue dissolved in DCM (30 mL), washed with sat. NH_4Cl (2×15 mL), sat. NaHCO, (2×15 mL), water (15 mL), and brine (15 mL). The organic layer was dried over $MgSO_4$, filtered and concentrated. Crude was recrystallized from ethyl acetate/hexane: The crude was dissolved in a minimum amount of hot ethyl acetate, hexane added to induce turbidity, gradually cooled to room temperature, then in an ice bath (0-5°C). Crystals 2a–2d were filtered, washed with cold hexane and dried under vacuum (22).

General method for the synthesis of (4-(((1H-indol-3-yl)methylene) amino) benzoyl)glutamic acid derivatives (3a-3h)

A 1.0 mmol solution of 2a–2h in DCM (9 mL) at 0–5 °C was treated dropwise with methanolic 3 N NaOH (1.0–1.2 mL, 3.0–3.6 mmol), giving a biphasic CH_2Cl_2: MeOH (9:1) mixture with 0.3–0.36 N alkali. The sodium carboxylate salt was obtained from the resulting solution as a white/off-white powder upon vigorous stirring at 0-5℃ for 60-90 min. TLC monitored completion. Ester consumption was followed by vacuum filtration of the salt and washing with cold DCM (10 mL) followed by reduced pressure drying. The solid was re-suspended in ice water, added acid (1N HCl) to pH 2-3, stirred for 5 min, filtered, washed with cold water and vacuum-dried (23). The chemical structure of the final synthesized compounds (3a-3h) are shown in table (1).

Table 1: The chemical structure of the target compounds

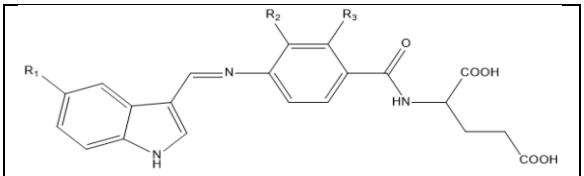

Compound code	R1	R2	R3
3a	H	H	H
3b	H	H	CH_3
3c	H	H	OCH_3
3d	H	Cl	H
3e	Br	H	H
3f	Br	H	CH_3
3g	Br	H	OCH_3
3h	Br	Cl	H

Spectral findings for the target compounds

Synthesis of (4-(((1H-indol-3-yl)methylene)amino)benzoyl) glutamic acid (3a)

The compound was synthesized according to the general synthetic procedure, % of Yield 87, Brown powder, mp: 206 ; IR (KBr, ν (cm^{-1}): 1612 (C=N, imine), 1652 (C=O, Amide), 1HNMR: (DMSO-d6, 400 MHz) δ = 12.18 (s, 2H, COOH), 10.93 (s, 1H, NH-indole), 9.03 (s, 1H, amide N-H), 8.69 (s, 1H, CH=N),8.20-8.29 (m, 2H, Ar-H), 8.08, 8.10 (d, 1H, Ar-H), 7.60, 7.62 (d, 1H, Ar-H), 7.48-7.53 (m, 2H, Ar-H), 7.20-7.28 (m, 2H, Ar-H), 4.02-4.09 (t, 1H, CH-NH), 2.42-2.57 (m, 2H, CH_2-COOH), 2.00-2.08 (m, 2H, CH_2-CH). ^{13}C NMR: (101 MHz, DMSO-d6) δ = 179.06 (1C, COOH), 172.15 (1C, COOH), 166.95 (1C, C(=O)-NH), 152.31 (1C, CH=N), 149.05, 138.99, 137.50, 13573, 131.69, 130.12, 123.93, 123.15, 122.61, 121.27, 118.59, 113.07, 112.91, 51.69, 29.43, 25.61.

Synthesis of (4-(((1H-indol-3-yl)methylene)amino)-2-methylbenzoyl)glutamic acid (3b)

The compound was synthesized according to the general synthetic procedure, % of Yield 79, Yellowish-Brown powder, mp: 210 ; IR (KBr, ν (cm^{-1}): 1608 (C=N, imine), 1651 (C=O, Amide), 1HNMR: (DMSO-d6, 400 MHz) δ = 12.20 (s, 2H, COOH), 11.09 (s, 1H, NH-indole), 9.04 (s, 1H, amide N-H), 8.69 (s, 1H, CH=N), 8.19-8.29 (m, 2H, Ar-H), 8.10 (s, 1H, Ar-H), 7.62, 7.64 (d, 2H, Ar-H), 7.53 (s, 1H, Ar-H), 7.20-7.28 (m, 2H, Ar-H), 4.04-4.10 (t, 1H, CH-NH), 2.44-2.58 (m, 2H, CH_2-COOH), 2.40 (s, 3H, CH_3), 2.02-2.09 (m, 2H, CH_2-CH). ^{13}C NMR: (101 MHz, DMSO-d6) δ = 177.45 (1C, COOH), 172.14 (1C, COOH), 168.67 (1C, C(=O)-NH), 156.54 (1C, CH=N), 149.08, 142.32, 138.94, 137.52, 135.72, 133.48, 130.17, 123.91, 121.28, 118.61, 116.43, 116.28, 112.90, 111.00, 53.50, 27.06, 24.15, 20.91.

Synthesis of (4-(((1H-indol-3-yl)methylene)amino)-2-methoxybenzoyl)glutamic acid (3c)

The compound was synthesized according to the general synthetic procedure, % of Yield 82, Dark-Brown powder, mp: 196 ; IR (KBr, ν (cm^{-1}): 1612 (C=N, imine), 1673 (C=O, Amide), 1HNMR: (DMSO-d6, 400 MHz) δ = 12.22 (s, 2H, COOH), 10.96 (s, 1H, NH-indole), 9.04 (s, 1H, amide N-H), 8.70 (s, 1H, CH=N), 8.22, 8.23 (d, 1H, Ar-H), 8.09, 8.10 (d, 1H, Ar-H), 7.61 (s, 1H, Ar-H), 7.49-7.51 (m, 2H, Ar-H), 7.19-7.28 (m, 2H, Ar-H), 6.98 (s, 1H, Ar-H), 4.05-4.09 (t, 1H, CH-NH), 3.73 (s,3H, OCH_3), 2.43-2.60 (m, 2H, CH_2-COOH), 2.01-2.09 (m, 2H, CH_2-CH). ^{13}C NMR: (101 MHz, DMSO-d6) δ = 177.71 (1C, COOH), 174.74 (1C, COOH), 169.58 (1C, C(=O)-NH), 161.61(1C, Ar-C), 155.02 (1C, CH=N), 152.33, 138.94, 137.52, 135.67, 134.32, 130.13, 123.89, 122.58, 121.27, 118.61, 112.90, 106.25, 106.06, 55.66, 51.66, 30.32, 25.63.

Synthesis of (4-(((1H-indol-3-yl)methylene)amino)-3-chlorobenzoyl) glutamic acid (3d)

The compound was synthesized according to the general synthetic procedure, % of Yield 75, Yellowish-Brown powder, mp: 232 ; IR (KBr, ν (cm^{-1}): 1612 (C=N, imine), 1652 (C=O, Amide), 1HNMR: (DMSO-d6, 400 MHz) δ = 12.24 (s, 2H, COOH), 11.24 (s, 1H, NH-indole), 9.05 (s, 1H, amide N-H), 8.70 (s, 1H, CH=N), 8.28, 8.29 (d, 1H, Ar-H), 8.21, 8.22 (d, 1H, Ar-H), 8.09, 8.11 (d, 1H, Ar-H), 7.72 (s, 1H, Ar-H), 7.59, 7.61 (d, 1H, Ar-H), 7.50, 7.51 (d, 1H, Ar-H), 7.19-7.28 (m, 2H, Ar-H), 4.04-4.09 (t, 1H, CH-NH), 2.42-2.60 (m, 2H, CH_2-COOH), 2.04-2.09 (m, 2H, CH_2-CH). ^{13}C NMR: (101 MHz, DMSO-d6) δ = 175.27 (1C, COOH), 172.15 (1C, COOH), 166.96 (1C, C(=O)-NH), 157.63 (1C, CH=N), 150.53, 138.93, 135.68, 131.09, 130.13, 129.97, 123.88, 122.58, 121.28, 118.79, 118.60, 116.40, 114.61, 112.91, 49.34, 27.05, 22.68.

Synthesis of (4-(((5-bromo-1H-indol-3-yl)methylene) amino)benzoyl)glutamic acid (3e)

The compound was synthesized according to the general synthetic procedure, % of Yield 76, Brown powder, mp: 224 ; IR (KBr, ν (cm^{-1}): 1604 (C=N, imine), 1638 (C=O, Amide), 1HNMR: (DMSO-d6, 400 MHz) δ = 12.45 (s, 2H, COOH), 11.09 (s, 1H, NH-indole), 9.04 (s, 1H, amide N-H), 8.70 (s, 1H, CH=N), 8.35 (s, 1H, Ar-H), 8.20-8.24 (m, 1H, Ar-H), 7.60, 7.62 (d, 1H, Ar-H), 7.48-7.52 (m, 1H, Ar-H), 7.38-7.41, 4.04-4.09 (t, 1H, CH-NH), 2.43-2.60 (m, 2H, CH_2-COOH), 2.03-2.09 (m, 2H, CH_2-CH). ^{13}C NMR: (101 MHz, DMSO-d6) δ = 172.15 (1C, COOH), 169.57 (1C, COOH), 167.97 (1C, C(=O)-NH), 153.62 (1C, CH=N), 149.14, 136.24, 135.65, 13168, 130.12, 126.50, 126.35, 123.87, 123.38, 117.87, 117.32, 115.28, 115.06, 113.03, 53.78, 29.50, 23.16.

Synthesis of (4-(((5-bromo-1H-indol-3-yl)methylene) amino)-2-methylbenzoyl)glutamic acid (3f)

The compound was synthesized according to the general synthetic procedure, % of Yield 84, Dark-Brown powder, mp: 218 ; IR (KBr, ν (cm^{-1}): 1606 (C=N, imine), 1652 (C=O, Amide), 1HNMR: (DMSO-d6, 400 MHz) δ = 12.36 (s, 2H, COOH), 11.07 (s, 1H, NH-indole), 9.03 (s, 1H, amide N-H), 8.69 (s, 1H, CH=N), 8.35 (s, 1H, Ar-H), 8.17-8.23 (m, 2H, Ar-H), 8.61, 8.63 (d, 2H, Ar-H), 7.50, 7.51 (d, 1H, Ar-H), 7.39 (s, 1H, Ar-H), 4.05-4.10 (t, 1H, CH-NH), 2.42-2.59 (m, 2H, CH_2-COOH), 2.40 (s, 3H, CH_3), 2.00-2.08 (m, 2H, CH_2-CH). ^{13}C NMR: (101 MHz, DMSO-d6) δ = 177.03 (1C, COOH), 173.48 (1C, COOH), 166.90 (1C, C(=O)-NH), 161.90 (1C, CH=N), 152.35, 142.31, 139.75, 136.23, 135.63, 133.48, 130.12, 126.52, 123.88, 123.38, 117.89, 115.28, 115.05, 110.93, 54.77, 29.47, 25.64, 22.77.

Synthesis of (4-(((5-bromo-1H-indol-3-yl)methylene) amino)-2-methoxybenzoyl)glutamic acid (3g)

The compound was synthesized according to the general synthetic procedure, % of Yield 71, Brown powder, mp: 231 ; IR (KBr, ν (cm^{-1}): 1608 (C=N, imine), 1633 (C=O, Amide), 1HNMR: (DMSO-d6, 400 MHz) δ = 12.37 (s, 2H, COOH), 10.91 (s, 1H, NH-indole), 9.03 (s, 1H, amide N-H), 8.70 (s, 1H, CH=N), 8.35 (s, 1H, Ar-H), 8.17-8.22 (m, 2H, Ar-H), 7.60 (s, 1H, Ar-H), 7.48-7.52 (m, 2H, Ar-H), 7.39 (s, 1H, Ar-H), 4.04-4.06 (t, 1H, CH-NH), 3.73 (s,3H, OCH_3), 2.42-2.59 (m, 2H, CH_2-

COOH), 1.99-2.08 (m, 2H, CH_2-CH). ^{13}C NMR: (101 MHz, DMSO-d6) δ = 179.15 (1C, COOH), 172.15 (1C, COOH), 169.61 (1C, C(=O)-NH), 155.021(1C, Ar-C), 149.13 (1C, CH=N), 139.76, 136.23, 135.63, 134.32, 130.12, 126.53, 126.35, 123.89, 123.38, 117.88, 115.06, 106.04, 55.66, 50.29, 28.27, 25.64.

Synthesis of (4-(((5-bromo-1H-indol-3-yl)methylene) amino)-3-chlorobenzoyl)glutamic acid (3h)

The compound was synthesized according to the general synthetic procedure, % of Yield 71, Yellow powder, mp: 243 ; IR (KBr, ν (cm^{-1}): 1608 (C=N, imine), 1643 (C=O, Amide), 1HNMR: (DMSO-d6, 400 MHz) δ = 12.38 (s, 2H, COOH), 11.14 (s, 1H, NH-indole), 9.03 (s, 1H, amide N-H), 8.69 (s, 1H, CH=N), 8.35 (s, 1H, Ar-H), 8.22 (s, 1H, Ar-H), 7.99, 8.01 (d, 1H, Ar-H), 7.70 (s, 1H, Ar-H), 7.58, 7.60 (d, 1H, Ar-H), 7.48, 7.50 (m, 1H, Ar-H), 7.39, 7.41 (d, 1H, Ar-H), 4.08-4.10 (t, 1H, CH-NH), 2.42-2.59 (m, 2H, CH_2-COOH), 2.02-2.08 (m, 2H, CH_2-CH). ^{13}C NMR: (101 MHz, DMSO-d6) δ = 178.76 (1C, COOH), 174.51 (1C, COOH), 169.61 (1C, C(=O)-NH), 157.56 (1C, CH=N), 149.34, 139.75, 136.23, 135.63, 131.08, 130.12, 129.97, 126.52, 123.89, 123.38, 118.77, 116.38, 115.06, 114.60, 53.65, 27.76, 23.46.

DFT study

The quantum chemistry package ORCA 6.1 was used for all DFT calculations. The hybrid meta-GGA B3LYP functional was used in combination with the Ahlrichs def2-SVP basis set for geometry optimizations, while the D3BJ dispersion correction was applied to consider non-covalent interactions. To ensure well converged stationary points, tight optimization convergence criteria (TightOpt) were used. The calculations were all done using the resolution-of-identity (RI) approximation and the def2/J auxiliary basis set. After full geometry optimization, the energies of the frontier molecular orbitals (FMOs) namely the highest occupied molecular orbital (HOMO) and the lowest unoccupied molecular orbital (LUMO) were obtained from the converged wavefunction. The global reactivity descriptors such as electronegativity (χ), electron affinity (EA), ionization potential (IP), chemical hardness (η), chemical potential (μ) and electrophilicity index (ω) were then calculated from these energies using the conceptual DFT formalism.

In silico drug-likeness and ADMET prediction

Prediction of the ADME and toxicology of the identified compounds were done in silico using the established Web-based tools. The SMILES of the compounds were entered into Swiss ADME, which allowed computing core physicochemical parameters, including molecular weight, logP, and topological polar surface area (TPSA) and provided a preliminary measure of drug-likeness (24,25).

MTT Methodology for MCF7 and MDA-MB-231

Cell viability was measured using the MTT (3-(4,5-dimethylthiazol-2-yl)-2,5-diphenyltetrazolium bromide) assay. Both MCF7 and MDA-MB-231 cells were plated in 96-well plates at a concentration of 1 × 104 cells/well and incubated for 24 hours. Following adherence, cells were treated with ten different concentrations (3.125, 6.25, 12.5, 25, 50, 100, 200, 400, 800, 1600 μM) of the designated compounds (MDA: 1a, 1b, 1e, 1h; MCF7: 1c, 1d, 1f, 1g). Acetazolamide and doxorubicin were used as positive controls for the MDA-MB-231 and MCF7 cell lines respectively, while DMSO was used as a negative control (up to 0.1% v/v). Triplicates of treatments and controls were set up. Cell viability was determined after 24 and 72 hours of treatment using the Promega CellTiter 96® AQueous One Solution Cell Proliferation Assay (MTS). In short, 20 μL of MTS reagent was added to the wells and the plates were incubated for 1-4 hours at 37°C. The absorbance of the formazan was measured at 490 nm using the GloMax® Explorer Multimode Microplate Reader (Promega) with a pre-validated protocol for absorbance measurements. The percentage of cell viability was calculated based on the DMSO control and the half-maximal inhibitory concentration (IC_{50}) was calculated from the dose-response curve.

RESULTS

Synthesis

The final compounds 3a-3h were synthesized as shown in scheme 1 and were verified by ^{1}H and ^{13}C-NMR. All ^{1}H-NMR spectra showed a distinct singlet around δ 8.69-8.70 ppm for the imine (CH=N) proton, a singlet at around δ 9.03-9.05 ppm for the amide N-H and a broad singlet at about δ 10.91-11.24 ppm for the indole N-H. The α-methine (CH-NH) of glutamic acid appeared as a triplet at δ 4.04-4.10 ppm, and the two diastereotopic methylene groups next to the carboxylic acid groups were

observed as a multiplets in the range of δ 2.00-2.60 ppm. The ^{13}C-NMR spectra also confirmed the structures, with expected signals for the two carboxylate carbon atoms (δ 172.15-179.15 ppm) and the amide carbon C(=O)–NH (δ 166.90-169.61 ppm).

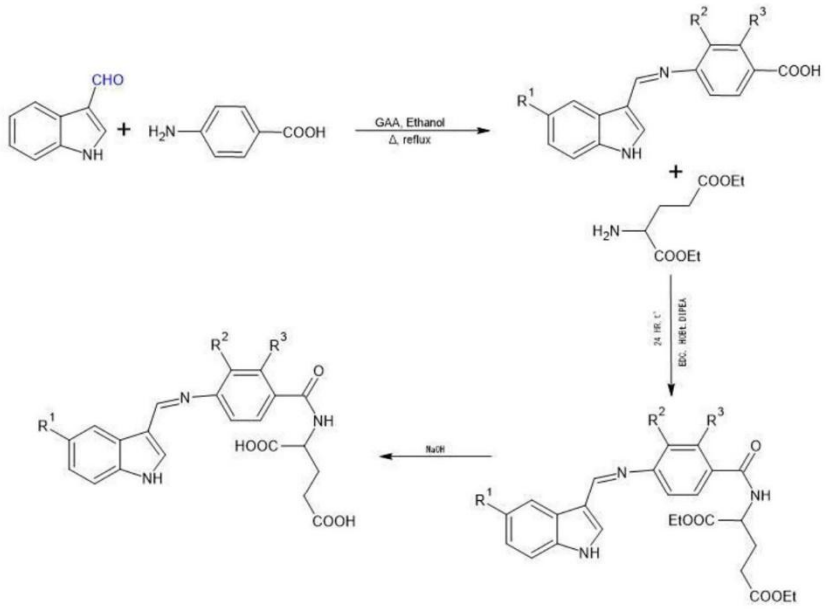

Scheme 1: Synthesis for the target compounds

DFT results

To rationalize the substituent effects on the frontier molecular orbital, global reactivity indexes, electronic structures and chemical characteristics of the synthesized ligands were carried out systematically by DFT calculation at the B3LYP-D3BJ/def2-SVP level of theory. Ligands with strong electron donating groups (e.g., compounds 1, 5, and 7) are highly electron-rich and polarizable with exceptionally narrow HOMO–LUMO gaps (0.528–0.616 eV) with positive HOMO and LUMO eigenvalues, which means very high chemical softness (S = 1.62–1.89 eV^{-1}) and very low chemical hardness (η = 0.26–0.31 eV). On the contrary, the electron withdrawing chlorine or the electron modulating methyl group (2, 3, 4, 6, 8) helps to stabilize the frontier orbitals leading to significant increase in energy gap (2.49–4.08 eV), negative chemical potential (μ = –3.75 to –4.32 eV), and hardness (η > 1.9 eV), indicating increased kinetic stability and electrostatic interaction tendency.

ADME results

The in silico ADME properties show that the developed compounds possess a generally good drug-like property, with majority of the derivatives fulfilling important physicochemical properties. All the compounds have Bioavailability Score of 0.56, which suggests moderate oral absorption potential, with low to moderate lipophilicity (LogP 2.14–3.38) and acceptable polar surface areas (TPSA 131.85–141.08 Å²). All compounds (1-6) satisfy Lipinski's Rule of Five (RO5), but compounds (7, 8) are only penalized for exceeding the molecular weight limit (>500 Da), which indicates that this could potentially come with a permeability penalty. There are no PAINS alerts throughout the series, however a universal prediction of poor blood-brain barrier penetration (BBB-P = No) suggests poor CNS accessibility.

***In vitro* cytotoxicity study**

IC50 data, defined as the concentration of the drug that inhibits 50% of the cell growth, shows that all the compounds tested have improved potency against both cancer cell lines, MDA and MCF-7 as time progresses (24h vs 72h). Compounds 3b and 3h showed the most potent activity against MDA cell line with IC50 values of 26.34 and 19.93 μM, respectively at 72 hour. Interestingly, the potency of 3h was seen to be better at the 72 h time point when compared with the reference drug Acetazolamide (AZM, IC50 = 24.98 μM). The most effective analog against MCF-7 cell line was 3f with an IC50 value of 28.56 μM after 72 hours. The dose-response curves for both cell lines are presented in figure 1.

Natural Resources for Human Health
eISSN: 2583-1194

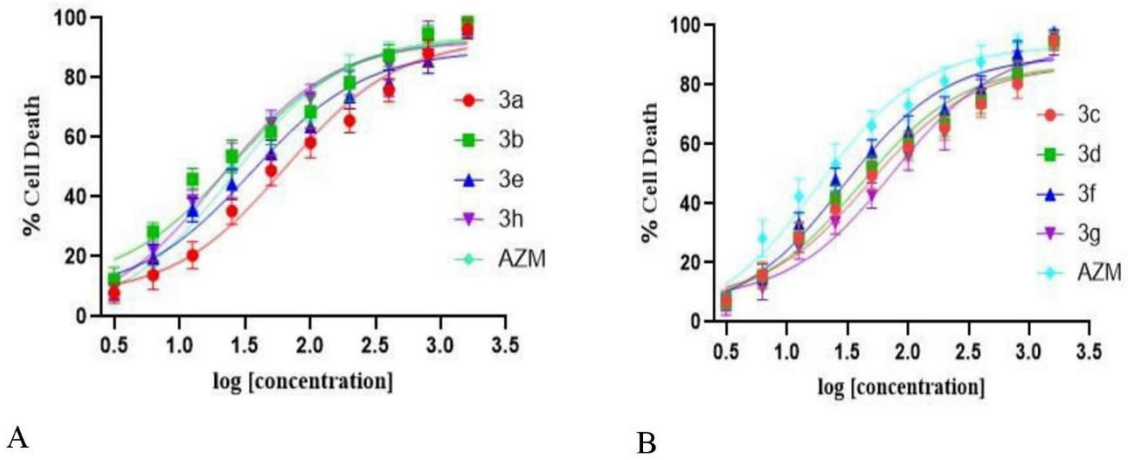

Figure 1: Dose-response curve of compounds and Acetazolamide against: a. MDA, and b: MCF-7 cell lines

The percentage of cell death data at a fixed concentration of 50 μM is used to obtain a measure of the cytotoxic efficacy of the compounds; the results in general support the IC50 data (Figure 2). All the compounds tested showed increase in the cell death with time in the MDA cell line with 3b (61.90%) and 3h (64.62%) being the most active as compared with the reference drug (Acetazolamide 61.49%). From this result, it can be seen that 3h and 3b are more effective in killing MDA cells at this concentration compared to the standard treatment. With MCF-7 cell line, 3f was again the most active compound, killing 57.61% of the cells after 72 hours, and the other derivatives (3c, 3d and 3g) exhibited moderate activity (42-52%). But the reference drug Acetazolamide was still better in this cell line with 66.29% cell death at 72 hours.

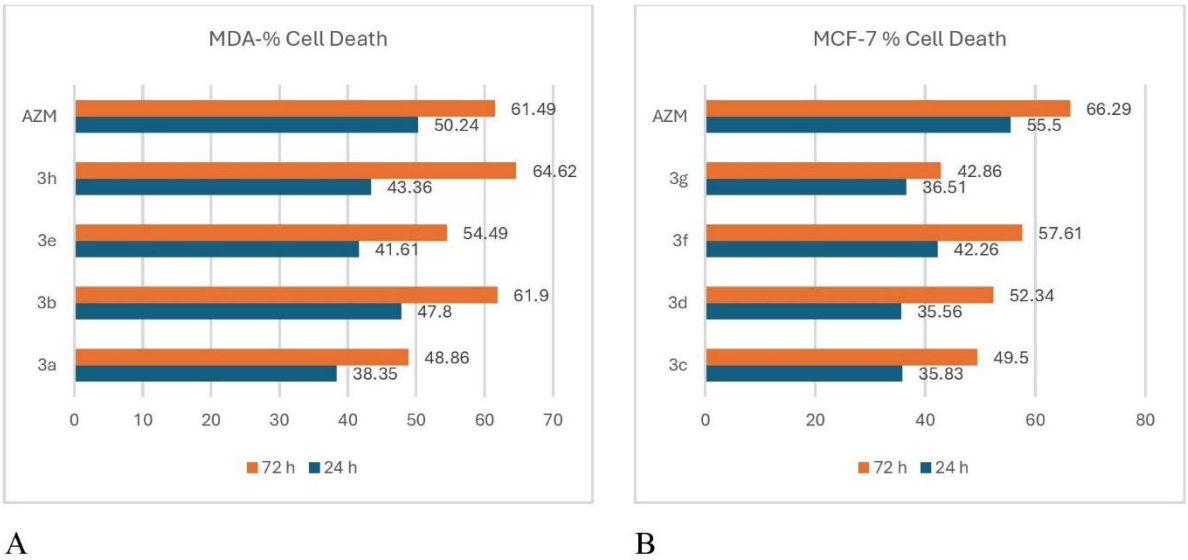

Figure 2: Cell death percentage of synthesized compounds and Acetazolamide against a. MDA and b. MCF-7 cell lines

DISCUSSION

The imine carbon (CH=N) resonated between δ 149.13-161.90 ppm, with minor variations due to the different substituents on the benzoyl and indole rings. Other expected aromatic and substituent carbon signals (e.g., methyl at δ 20.91 ppm, methoxy at δ 55.66 ppm, brominated aromatic carbons) were also present, confirming the successful synthesis of all desired compounds. These structural features along with the characteristic ^{1}H NMR and ^{13}C NMR signals confirm the proposed structure of the synthesized compounds. The differential reactivity and coordination modes experienced in the synthesis of the corresponding metal complexes can be understood on the basis of an electronic dichotomy that can be explained quantitatively by the substituents. It is important to note that, among those descriptors, the chemical hardness, electrophilicity index, are intrinsic electronic properties that will be used as basis to rationalize bioactive conformations and interactions with the targets that the

free ligands form in our next computational investigation. From the overall ADME results, it can be seen that compounds 1–6 are druggable, and the heavier analogues (7 and 8) might need to be further optimized to increase the compounds' pharmacokinetic suitability. Compounds 1–6 have favorable physicochemical characteristics which encourage their further evaluation as potential drug candidates, while compounds 7 and 8 may require structural optimization as their molecular weights are slightly above that imperative optimum oral bioavailability. The MTT test findings confirm the excellent activity of compounds 3h and 3b towards MDA cells and 3f is the most active compound towards MCF-7 cells showing cell-killing potential reaching towards the standard drug. All of the synthesized compounds were however less active than the reference standard Acetazolamide which was found to be highly potent against MCF-7 cells with IC50 of 18.08 μM at 72 hours. Based on the overall results, the compounds have shown greater activity against the MDA cell line as compared to the MCF-7 cell line with the 3b and 3h scaffolds showing the highest activity. These outcomes suggest that the synthesized compounds exhibit varying degrees of cytotoxic activity across the breast cancer cell lines tested. Among them, compounds 3b and 3h showed the strongest activity against MDA cells, whereas compound 3f exhibited the highest activity against MCF-7 cells.

CONCLUSION

Eight novel indole-PABA hybrids have been designed and synthesized as multi-target inhibitors of hDHFR and carbonic anhydrase IX/XII for breast cancer therapy with success. The synthetic route developed was Schiff base formation, peptide coupling and alkaline hydrolysis, yielding the target compounds in 71-87% yields, whose structures were confirmed by spectroscopy. The in silico ADMET profile indicated good drug-like properties of the compounds, where compounds 3a to 3f met Lipinski's Rule of Five and DFT calculations gave insight into the substituent-dependent electronic reactivity. The 3-chloro derivative (3h) had the strongest cytotoxicity on triple-negative breast cancer cells (MDA-MB-231) (IC_{50} = 19.93 μM) after 72 h and the 5-bromo-2-methyl analog (3f) was the most potent on hormone receptor positive cells (MCF-7) (IC_{50} = 28.56 μM) under the same conditions. Substitution of the 3-chloro and 5-bromo atoms by halogen seemed to give some promise for potency. The compounds 3h, 3b and 3f were the most promising ones with moderate drug-like properties. The results presented here serve as a strong basis to pursue further optimization of the above compound such as enzyme inhibition assays, mechanistic studies as well as in vivo studies to further progress the field of multi-targeted breast cancer therapies.

Declaration of Competing Interest

There are no conflicts to declare

Acknowledgement

The authors gratefully acknowledge Mustansiriyah University (www.uomustansiriyah.edu.iq) in Baghdad, Iraq, for their assistance in finishing this work.

REFERENCES

[1] Xiong X, Zheng LW, Ding Y, Chen YF, Cai YW, Wang LP, et al. Breast cancer: pathogenesis and treatments. Signal Transduct Target Ther. 2025 Feb 19; 10(1):49. doi:10.1038/s41392-024-02108-4
[2] Giaquinto AN, Sung H, Miller KD, Kramer JL, Newman LA, Minihan A, et al. Breast Cancer Statistics, 2022. CA Cancer J Clin. 2022 Nov; 72(6):524–41. doi:10.3322/caac.21754
[3] Kim J, Harper A, McCormack V, Sung H, Houssami N, Morgan E, et al. Global patterns and trends in breast cancer incidence and mortality across 185 countries. Nat Med. 2025 Apr; 31(4):1154–62. doi:10.1038/s41591-025-03502-3
[4] Hong R, Xu B. Breast cancer: an up-to-date review and future perspectives. Cancer Commun. 2022 Oct; 42(10):913–36. doi:10.1002/cac2.12358
[5] Obeagu EI, Obeagu GU. Breast cancer: A review of risk factors and diagnosis. Medicine (Baltimore). 2024 Jan 19; 103(3):e36905. doi:10.1097/MD.0000000000036905
[6] Kim J, Munster PN. Estrogens and breast cancer. Ann Oncol. 2025 Feb;36(2):134–48. doi:10.1016/j.annonc.2024.10.824
[7] Wang J, Wu SG. Breast Cancer: An Overview of Current Therapeutic Strategies, Challenge, and Perspectives. Breast Cancer Targets Ther. 2023 Oct; 15: 721–30. doi:10.2147/BCTT.S432526.
[8] Ye F, Dewanjee S, Li Y, Jha NK, Chen ZS, Kumar A, et al. Advancements in clinical aspects of targeted therapy and immunotherapy in breast cancer. Mol Cancer. 2023 Jul 6; 22(1):105. doi:10.1186/s12943-023-01805-y
[9] Zagami P, Carey LA. Triple negative breast cancer: Pitfalls and progress. Npj Breast Cancer. 2022 Aug 20; 8(1):95. doi:10.1038/s41523-022-00468-0

[10] Dos-Santos-Silva I, Gupta S, Orem J, Shulman LN. Global disparities in access to cancer care. Commun Med. 2022 Apr 7; 2(1): 31. doi:10.1038/s43856-022-00097-5
[11] Doostmohammadi A, Jooya H, Ghorbanian K, Gohari S, Dadashpour M. Potentials and future perspectives of multi-target drugs in cancer treatment: the next generation anti-cancer agents. Cell Commun Signal. 2024 Apr 15; 22(1):228. doi:10.1186/s12964-024-01607-9
[12] Bi X, Wang Y, Wang J, Liu C. Machine Learning for Multi-Target Drug Discovery: Challenges and Opportunities in Systems Pharmacology. Pharmaceutics. 2025 Sep 12; 17(9):1186. doi:10.3390/pharmaceutics17091186
[13] Abdelsayed M. AI-Driven Polypharmacology in Small-Molecule Drug Discovery. Int J Mol Sci. 2025 Jul 21; 26(14):6996. doi:10.3390/ijms26146996
[14] Noce B, Di Bello E, Fioravanti R, Mai A. LSD1 inhibitors for cancer treatment: Focus on multi-target agents and compounds in clinical trials. Front Pharmacol. 2023 Feb 2; 14: 1120911. doi:10.3389/fphar.2023.1120911
[15] Amaral C, Almeida CF, Valente MJ, Varela CL, Costa SC, Roleira FMF, et al. New Promising Steroidal Aromatase Inhibitors with Multi-Target Action on Estrogen and Androgen Receptors for Breast Cancer Treatment. Cancers. 2025 Jan 7; 17(2): 165. doi:10.3390/cancers17020165
[16] Rudrapal M, Paudel KR, Pangeni R. Editorial: Drug repurposing and polypharmacology: A synergistic approach in multi-target based drug discovery. Front Pharmacol. 2022 Dec 20; 13: 1101007. doi:10.3389/fphar.2022.1101007
[17] Galassi R, Luciani L, Gambini V, Vincenzetti S, Lupidi G, Amici A, et al. Multi-Targeted Anticancer Activity of Imidazolate Phosphane Gold(I) Compounds by Inhibition of DHFR and TrxR in Breast Cancer Cells. Front Chem. 2021 Jan 11; 8: 602845. doi:10.3389/fchem.2020.602845
[18] Brown JI, Wang P, Wong AYL, Petrova B, Persaud R, Soukhtehzari S, et al. Cycloguanil and Analogues Potently Target DHFR in Cancer Cells to Elicit Anti-Cancer Activity. Metabolites. 2023 Jan 19; 13(2):151. doi:10.3390/metabo13020151
[19] Numprasit W, Yangngam S, Prasopsiri J, Quinn JA, Edwards J, Thuwajit C. Carbonic anhydrase IX-related tumoral hypoxia predicts worse prognosis in breast cancer: A systematic review and meta-analysis. Front Med. 2023 Mar 17; 10: 1087270. doi:10.3389/fmed.2023.1087270
[20] Dolatkhah M, Omidi Y. Renewed interests in carbonic anhydrase IX in relevance to breast cancer treatment. BioImpacts. 2019 Aug 27; 9(4): 195–7. doi:10.15171/bi.2019.24
[21] Wang C, Fan L, Pan Z, Fan S, Shi L, Li X, et al. Synthesis of Novel Indole Schiff Base Compounds and Their Antifungal Activities. Molecules. 2022 Oct 13; 27(20): 6858. doi:10.3390/molecules27206858
[22] Xu Q, Xie Y, Qi J, Ren Z, Coluccini C, Coghi P. Development of New Amide Derivatives of Betulinic Acid: Synthetic Approaches and Structural Characterization. Molbank. 2025 Oct 13; 2025(4): M2072. doi:10.3390/M2072
[23] Theodorou V, Alagiannis M, Ntemou N, Brentas A, Voulgari P, Polychronidou V, et al. Mild alkaline hydrolysis of hindered esters in non-aqueous solution. Arkivoc. 2018 Oct 27; 2018(7): 308–19. doi:10.24820/ark.5550190.p010.673
[24] Sumia Samer Tayah, Shakir Mahmood Alwan, Kenza Mansoor. In Silico Profiling of Binding Affinities of Hybrid Molecules of Oseltamivir carboxamides cross-linked with Hydroxamic acid as possible Anti-influenza agents. Al Mustansiriyah J Pharm Sci. 2025 May 7; 25(2): 170–8. doi:10.32947/ajps.v25i2.1133
[25] Sarmad Abbas Fadhil, Karima Fadhil Ali, Wesen Adel Mehde. In-Silico Evaluation of Binding Interaction and ADME Properties of Novel Pyrazoline and Pyrimidine Derivatives Targeting Cyclooxygenase-2 Enzyme. Al Mustansiriyah J Pharm Sci. 2025 Jan 14; 25(1): 110–30. doi:10.32947/ajps.v25i1.1148